AAS 16-253

A GNC SIMULATION OF A FAR-RANGE APPROACH TOWARDS A TARGET IN GEOSTATIONARY ORBIT

Sofya Spiridonova[*] and Ralph Kahle[†]

This paper describes a GNC simulation as part of a feasibility analysis conducted by DLR/GSOC for future on-orbit servicing missions in near-geostationary orbit. The simulation addresses a far-range approach from several kilometers down to a few hundred meters, which includes relative orbit determination based on simulated optical measurements, and autonomous maneuver planning for relative trajectory control. One hundred simulation runs are performed with varying initial conditions based on the expected absolute orbit determination errors prior to the approach initiation. The safety of the formation is granted, as the servicer satellite never enters a pre-defined collision-avoidance area around the target spacecraft.

The results of the simulation show that a low-cost far range approach based on optical measurements is feasible up to a safe transition to a mid-range sensor. The results of the paper as well as the proposed GNC algorithm itself can find applications in future on-orbit servicing missions in near-geostationary orbit.

INTRODUCTION

As the fleet of geostationary satellites is growing and the number of available longitude slots remains limited, developments in the field of On-Orbit Servicing (OOS) in geostationary orbit (GEO) including client spacecraft life extension, payload modification and active removal of old uncooperative satellites are becoming more and more important. In this context, a feasibility analysis was conducted by the German Space Operations Center (GSOC) in order to come up with a sensor concept and a Guidance, Navigation and Control (GNC) strategy that would allow a safe approach to a client satellite located in GEO.[3] At the same time, the know-how acquired by GSOC in the field of low Earth-orbit spacecraft formation flight was meant to be re-used whenever possible.[2,6,9]

As part of this framework, the present paper addresses major flight dynamics aspects of a safe far range approach towards a target in GEO, with an optical camera being the primary sensor. Azimuth and elevation of the Client as seen by the Servicer in the orbital frame are simulated based on the numerically integrated "true" reference trajectories of the two satellites. Expected errors due to sideways Sun illumination as well as the image processing noise are included into the measurement simulation. The determination of the relative position is done via batch least-squares parameter estimation, where the design of the navigation filter was inherited from the ARGON experiment on PRISMA mission.[7,8] For the safety of the formation, the concept of eccentricity and inclination vector separation[11] is used allowing passive collision prevention in the presence of large tangential uncertainties which are typical for angles-only navigation. A collision-avoidance region is defined around the Client that the Servicer shall not enter at any time.

[*]PhD, DLR, German Space Operations Center, Münchener Str. 20, 82234, Germany; E-mail: sofya.spiridonova@dlr.de
[†]Dr., DLR, German Space Operations Center, Münchener Str. 20, 82234, Germany; E-mail: ralph.kahle@dlr.de

During every phase of the approach, which spans relative distances from several kilometers to a few hundred meters, a relative orbit determination based on a stack of collected angular measurements is followed by a maneuver planning activity. A tangential relative drift correction maneuver is executed immediately after that in order to maintain the desired number of total drift orbits and counteract perturbations not taken into account by the relative motion model. Two radial maneuvers and two out-of-plane maneuvers are executed daily each at its optimal argument of latitude to allow a controlled step-wise reduction of the relative separation in the plane orthogonal to the flight direction.

To ensure that the developed GNC strategy complies with the safety requirements, one hundred simulation runs are performed with varying initial conditions based on the expected absolute orbit determination errors prior to the approach initiation. It is demonstrated, that the safety threshold in the plane perpendicular to the flight direction is never violated. The angles-only navigation solution proves sufficiently accurate to allow a safe approach towards the Client down to a few hundred meters where a transition to a mid-range sensor (e.g. a camera with a wider field-of-view for pose estimation) is possible in a time non-critical manner. Additionally, the paper provides an assessment of the overall performance of the GNC algorithm up to the acquisition of the final delivery geometry.

Formation safety as the main GNC design driver

One of the main requirements to consider while setting the boundary constraints and elaborating the GNC design is the guaranteed safety of the formation at any time. With the scope of this research being restricted to far range only, the concept of formation safety is based on the relative eccentricity and inclination vector separation. In the presence of large uncertainties in the along-track separation inherent to Angles-Only-Navigation (AON), the collision risk is measured as a function of the separation in the plane orthogonal to the flight direction. To ensure the safety of the formation, the projection of the relative position vector onto the normal plane should never be smaller than a predefined threshold, determined by the size of the two satellites and the relative navigation errors.

In the beginning of the far range approach, the expected relative navigation errors can be derived from the typical errors of absolute Orbit Determination (OD), performed using radar or optical tracking measurements. Current research on optical tracking techniques shows that the maximum errors of the absolute OD are restricted in in-flight and normal directions to 300 meters, and 260 meters in radial direction.[13] Since many optical tracking campaigns will be performed in the days before the ”go” for the approach initiation is given, these estimates are quite conservative. More optimistic estimates based on the experience collected at DLR GSOC were used for simulation initialization.

On the other hand, the definition of the target relative orbit at the end of the far range approach should take into account the dimensions of the two S/C as well as the expected errors of the last angles-only Relative Orbit Determination (ROD). The relatively large dimensions of typical telecommunication satellites and, in particular, the extensive solar arrays require the safety threshold in the cross-track plane of at least 50 meters.

After the switch-over to the mid-range sensor, reliable measurements of the relative separation should be available, allowing a reduction of the separation in the plane perpendicular to the flight direction to zero for forced-motion phase initiation.

It should be noted that the described safety criteria and the requirement of keeping the Client in

the Field of View (FOV) of a typical far range camera would be impossible to fulfill simultaneously without an active steering of the Servicer. A simple calculation proves that to keep the Client in the FOV of 10 degrees of a typical far range camera with the bore-sight fixed in flight direction, the separation in the normal plane should not exceed 435 m at the distance of 5 km, and 17 m at the distance of 300 m. This would violate the safety constraint, and therefore, the capability of the Servicer to perform target tracking along the whole trajectory is essential.

RELATIVE MOTION DYNAMICS

Relative orbital elements

The relative motion of two close spacecraft can be characterized in terms of the following set of Relative Orbital Elements (ROEs)[5]

$$\delta\boldsymbol{\alpha} = \begin{pmatrix} \delta a \\ \delta\lambda \\ \delta e_x \\ \delta e_y \\ \delta i_x \\ \delta i_y \end{pmatrix} = \begin{pmatrix} (a_s - a_c)/a_s \\ (u_s - u_c) + (\Omega_s - \Omega_c)\cos i_s \\ e_{x,s} - e_{x,c} \\ e_{y,s} - e_{y,c} \\ i_s - i_c \\ (\Omega_s - \Omega_c)\sin i_s \end{pmatrix}, \tag{1}$$

where the non-singular elements

$$\begin{aligned} \boldsymbol{\kappa} &= (a, u, e_x, e_y, i, \Omega)^{\mathrm{T}} \\ &= (a, \omega + M, e\cos\omega, e\sin\omega, i, \Omega)^{\mathrm{T}} \end{aligned} \tag{2}$$

parametrize the absolute orbit of a single satellite. Here a, e, i, Ω, ω, M are the classical Keplerian elements, $u = \omega + M$ is the argument of latitude, and the subscripts s and c refer to the Servicer and the Client. Vectors $\delta\boldsymbol{e} = (\delta e_x, \delta e_y)^T$ and $\delta\boldsymbol{i} = (\delta i_x, \delta i_y)^T$ are called the relative eccentricity and the relative inclination vectors with magnitudes denoted by δe and δi, respectively.

All the absolute orbital elements that appear in the following refer to those of the Servicer satellite, therefore the subscript s is dropped.

Multiplied by the semi-major axis, the above ROEs allow a convenient representation of the ideal relative in-plane and out-of-plane motion.[5] Namely, under the assumptions of near-circular orbits and small spacecraft separations, the relative motion is bounded, if the offset in the semi-major axes $a\delta a$ is zero. In the orbital plane, the Servicer circumscribes with respect to the Client an ellipse with semi-major axis $2a\delta e$ in along-track direction and semi-minor axis $a\delta e$ in radial direction, whereas the amplitude of the oscillation in the direction orthogonal to the orbital plane is equal to $a\delta i$, Figure 1. The average relative offsets in the along-track and radial directions are equal to $a\delta\lambda$ and $a\delta a$, respectively.

More precisely, the following approximative linear relation between ROEs and the Cartesian relative state applies based on the equivalence of ROE and the integration constants in Hill-Clohessy-Wiltshire (HCW) equations[4] governing unperturbed relative motion.

$$\begin{pmatrix} \delta\boldsymbol{r}_{\mathrm{RTN}} \\ \delta\boldsymbol{v}_{\mathrm{RTN}} \end{pmatrix} = \boldsymbol{A} \cdot a\delta\boldsymbol{\alpha}, \tag{3}$$

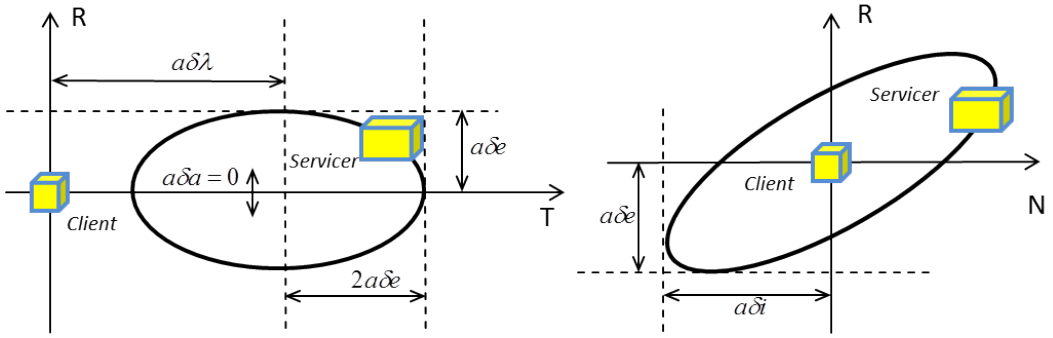

Figure 1. Unperturbed relative motion in the orbital plane (left) and in the plane perpendicular to the flight direction (right)

where

$$\boldsymbol{A} = \begin{pmatrix} 1 & 0 & -\cos u & -\sin u & 0 & 0 \\ 0 & 1 & 2\sin u & -2\cos u & 0 & 0 \\ 0 & 0 & 0 & 0 & \sin u & -\cos u \\ 0 & 0 & n\sin u & -n\cos u & 0 & 0 \\ -1.5n & 0 & 2n\cos u & 2n\sin u & 0 & 0 \\ 0 & 0 & 0 & 0 & n\cos u & n\sin u \end{pmatrix}.$$

Relative motion model

A Relative Motion Model (RMM) for relative state propagation within the ROD module is assumed to be implemented "aboard" the Servicer. First obtained in Reference 5, this RMM has been employed since then at GSOC in various Low-Earth-Orbit (LEO) formation-flying experiments,[6–8] and also forms the basis of the TanDEM-X Autonomous Formation Flying system.[1,2]

In the absence of maneuvers in the time interval $[t, t+\Delta t]$, the evolution of ROEs within this RMM can be formulated as

$$a\delta\boldsymbol{\alpha}(t+\Delta t) = \left(\boldsymbol{\Phi}_{\mathrm{HCW}}\left(\boldsymbol{\kappa}, \Delta t\right) + \boldsymbol{\Phi}_{J_2}\left(\boldsymbol{\kappa}, \Delta t\right)\right) \cdot a\delta\boldsymbol{\alpha}(t) \tag{4}$$

Here the sum of the state transition matrices

$$\boldsymbol{\Phi}_{\mathrm{HCW}} = \begin{pmatrix} 1 & 0 & 0 & 0 & 0 & 0 \\ -\frac{3}{2}n\Delta t & 1 & 0 & 0 & 0 & 0 \\ 0 & 0 & 1 & 0 & 0 & 0 \\ 0 & 0 & 0 & 1 & 0 & 0 \\ 0 & 0 & 0 & 0 & 1 & 0 \\ 0 & 0 & 0 & 0 & 0 & 1 \end{pmatrix}$$

and

$$\boldsymbol{\Phi}_{J_2} = n\Delta t \begin{pmatrix} 0 & 0 & 0 & 0 & 0 & 0 \\ -\frac{21}{4}\gamma H(\eta+1) & 0 & 0 & 0 & -\frac{3}{2}\gamma\sin 2i(3\eta+4) & 0 \\ 0 & 0 & 0 & -\varphi' & 0 & 0 \\ 0 & 0 & \varphi' & 0 & 0 & 0 \\ 0 & 0 & 0 & 0 & 0 & 0 \\ -\frac{21}{4}\gamma\sin 2i & 0 & 0 & 0 & 3\gamma\sin^2 i & 0 \end{pmatrix},$$

where $\eta = \sqrt{1-e^2}$, $H = 3\cos^2 i - 1$, $\varphi' = \frac{3}{2}\gamma\left(5\cos^2 i - 1\right)$, $\gamma = \frac{J_2}{2}\left(\frac{R_E}{a}\right)^2 \frac{1}{(1-e^2)^2}$, $J_2 \approx 1.082 \cdot 10^{-3}$ and R_E is the Earth equatorial radius, describes the evolution of ROEs in the time span of Δt under the influence of the oblate Earth. Under the assumptions of the Hill-Clohessy-Wiltshire (HCW) equations, the only relative element changing with time is the relative mean longitude $a\delta\lambda$. Namely, if the semi-major axis offset $a\delta a$ is not zero, the Servicer is drifting with respect to the Client with a rate of -3$\pi a\delta a$ per revolution. At the same time, main secular perturbations of bounded relative motion resulting from the Earth equatorial bulge can be summarized as a rotation of the relative eccentricity vector $a\delta\boldsymbol{e}$, a vertical drift of the relative inclination vector $a\delta\boldsymbol{i}$, and an additional drift of the relative mean argument of longitude $a\delta\lambda$. A detailed analysis of the unperturbed motion and the perturbations due to J_2 including the derivation of the matrix $\boldsymbol{\Phi}_{J_2}$ can be found in Reference 5.

In Reference 12, an extension of the RMM in Eq. 4 was proposed including the perturbations in ROEs due to the Solar Radiation Pressure (SRP), and the third-body gravitational perturbations. An integration of the extended RMM into the proposed GNC algorithm could potentially be of interest for future applications, but it is out of scope of the present paper, as the accuracy of the basic RMM is sufficient for the purpose of the present analysis.

Maneuver handling

The inversion of Eq. (3) under the assumption

$$\delta\boldsymbol{r}_{\mathrm{RTN}} = \mathbf{0}$$

provides a direct relation between an instantaneous velocity increment and the consequent change in ROEs at the epoch of the maneuver.

$$a\Delta\delta\boldsymbol{\alpha}_{\mathrm{M}} = \frac{1}{n}\begin{pmatrix} +2\delta v_T \\ -2\delta v_R \\ +\delta v_R \sin u_{\mathrm{M}} + 2\delta v_T \cos u_{\mathrm{M}} \\ -\delta v_R \cos u_{\mathrm{M}} + 2\delta v_T \sin u_{\mathrm{M}} \\ \delta v_N \cos u_{\mathrm{M}} \\ \delta v_N \sin u_{\mathrm{M}} \end{pmatrix}.$$

While RMM is applied for ROEs propagation in between of the maneuvers, instantaneous changes in ROEs induced by each impulsive maneuver in the interval from epoch t to epoch $t+\Delta t$ are added to the RMM-based propagation result under consideration of the specific epoch of any particular maneuver.

Figure 2 illustrates the described procedure, with t_{M-} denoting the epoch right before the epoch t_M of an impulsive maneuver and t_{M+} being the epoch right after the maneuver.

GNC DESIGN

Relative navigation concept

The determination of the relative position is based on batch least-squares estimation with a priori information, where the goal is to find the trajectory which minimizes the sum of the squared differences between the modeled observations and the "true" measurements. The employed navigation algorithm is based on the research of G. Gaias and J.-S. Ardeans (Reference 8).

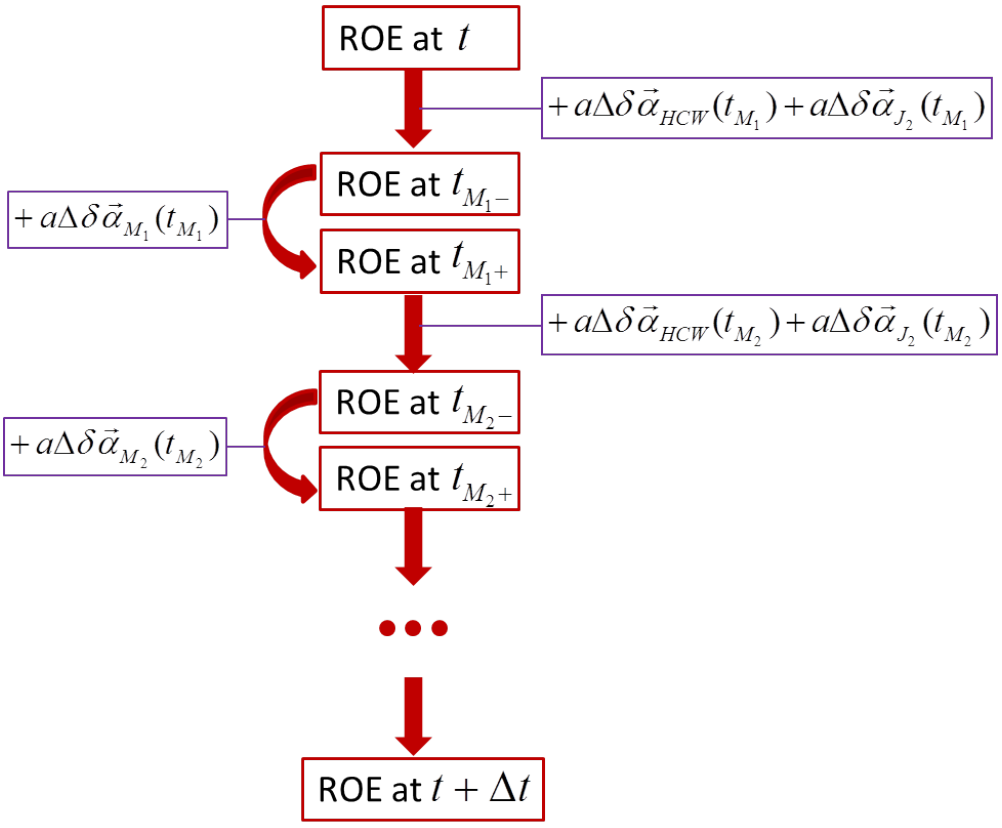

Figure 2. Maneuver handling

Let us assume that the epoch of the first relative orbit determination is t_0. The values obtained through the absolute orbit determination represent a priori information. This initial guess can be corrected in several iterations until the trajectory which best fits the measurements is found. The experience gained during the present simulations suggests that batches of 540 Line-of-Sight (LOS) measurements spanning 30 hours (i.e. one LOS measurement every 6.5 minutes) allow the optimal performance of the filter. The solution of the filter at t_0 is propagated according to RMM taking into account the performed maneuvers until the next epoch t_1, where it represents the new a priori information. Analogously, the solution obtained at t_1 is propagated according to RMM to serve as a priori information at epoch t_2.

Relative orbit determination can be repeated every several hours using the newly available measurements. Provided that enough maneuvers are executed along the trajectory, the error introduced by the initial absolute orbit determination can be gradually eliminated, so that the solution becomes more and more accurate as the Servicer approaches the Client.

Spiral approach with coupled guidance and control

The basic idea of the approach is the reduction of the relative mean longitude through enforcement of a constant non-zero relative semi-major axis. While approaching, the size of the relative ellipse in the plane orthogonal to the flight direction is gradually reduced by radial and normal maneuvers

performed twice a day after a relative orbit determination. The relative semi-major axis is kept at the optimal value through drift correction maneuvers designed to account for the perturbations such as the differential solar radiation pressure and the third-body differential perturbations which are neglected in the RMM. The relative orbit reduction phase is followed by a drift-stop maneuver which allows at the same time the final reduction of the relative eccentricity vector. Since the relatively large drift termination maneuver improves substantially the quality of the angles-only relative navigation solution, another ROD is performed and used for the final correction of the possible non-zero drift. The far range approach consists therefore of the 4 following phases.

- Relative drift initiation based on the absolute navigation solutions from radar or optical tracking measurements. For calculation of the required tangential Delta-V the optimal offset in the semi-major axis is defined by the initial and target along-track separation and the desired number of drift orbits, which is currently set to 4.5 orbits. Drift initiation maneuver is performed at an optimal argument of latitude to perform the first reduction of the radial component of the relative ellipse.

- Relative orbit reduction phase. The proposed concept suggests 4.5 drift orbits during which ROD is performed every 3-4 hours followed by a drift correction maneuver. The first ROD takes place 15 minutes after the drift initiation maneuver. The improvement of the AON observability properties consequent to the large tangential maneuver is, however, subject to a certain latency. Namely, the improvement of AON solution is best visible several hours after the drift initiation maneuver, when the attained change in LOS profile becomes more apparent. In the meantime, radial and normal relative orbit reduction maneuvers are planned after each ROD and executed if scheduled before the next ROD. Maneuvers scheduled for a later time are corrected after the next ROD. This control strategy results in a daily execution of two radial and two normal maneuvers performed each at its optimal argument of latitude.

- Drift termination on the intermediate target relative orbit. The intermediate orbit is introduced into the approach algorithm to fulfill the safety constraint in the absence of large maneuvers during the drift phase and the consequent degradation of the AON observability properties.

- Ultimate corrections phase. Last ROD after half a day of measurement collection is followed by the final corrections towards the nominal target relative orbit. This includes a zero-drift correction maneuver, as well as a radial and a normal maneuver performed each at the optimal argument of latitude. This phase can extend the overall duration of the operations by one day at most; however, it provides an essential improvement to the final relative orbit solution accuracy. In particular, the stability of the final achieved geometry, which requires $a\delta a = 0$, is crucial for a safe and time non-critical transition to mid-range camera as a primary sensor.

  It also has to be noted, that due to the coupling of relative eccentricity and relative mean longitude control, the last radial maneuver for relative eccentricity vector correction inevitably degrades the achieved accuracy in mean along-track separation $a\delta\lambda$. As a result, the final along-track separation might have a deviation of up to ± 100 m with respect to the target along-track separation of the nominal delivery geometry. None the less, the control of the relative ellipse in the plane orthogonal to the flight direction is prioritized over the control of the mean along-track separation, as long as a safe approach to the point where range measurements are possible is granted.

In total the duration of the far range approach can range from 5 to 6 days, which is considered acceptable under operational constraints. In Figure 3 and Figure 4, the nominal approach trajectory in the absence of absolute and relative orbit determination errors is illustrated by a 3D view and the subplots of projections of the relative position vector onto the planes formed by the radial / tangential, radial / normal and normal / tangential directions.

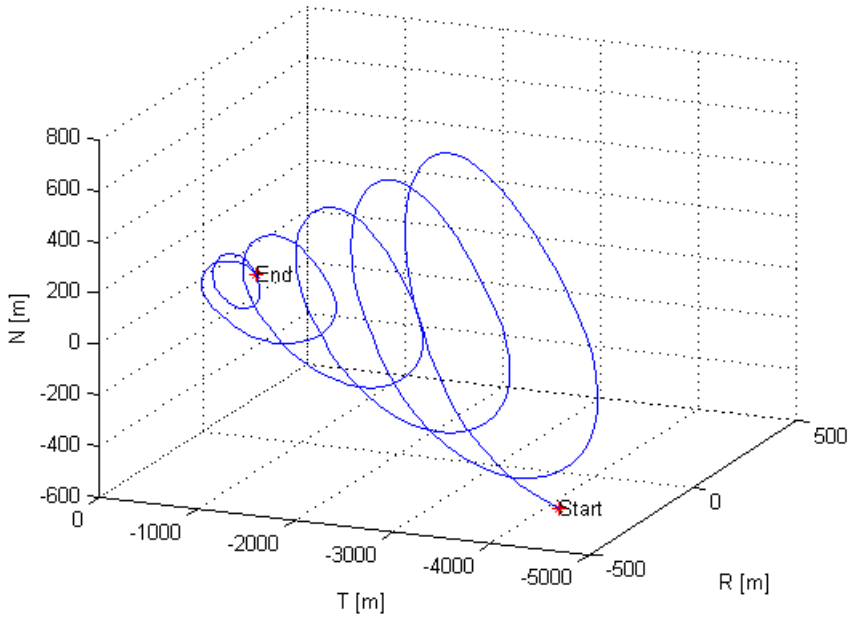

Figure 3. Nominal spiral approach in the absence of errors: 3D view.

SIMULATION SET-UP AND IMPLEMENTATION

Boundary conditions

Based on the requirement analysis, the following nominal initial formation geometry was selected for the beginning of the far range approach:

- Zero along-track drift: $a\delta a = 0$ m,
- Mean along-track separation of 3500 m: $a\delta\lambda = -3500$ m,
- Amplitude of radial oscillation of 500 m: $a\delta e_x = 0$ m, $a\delta e_y = 500$ m.
- Amplitude of cross-track oscillation of 700 m: $a\delta i_x = 0$ m, $a\delta i_y = 700$ m.

The nominal target formation geometry to be achieved at the end of the far range phase was defined as follows:

- Zero along-track drift: $a\delta a = 0$ m,

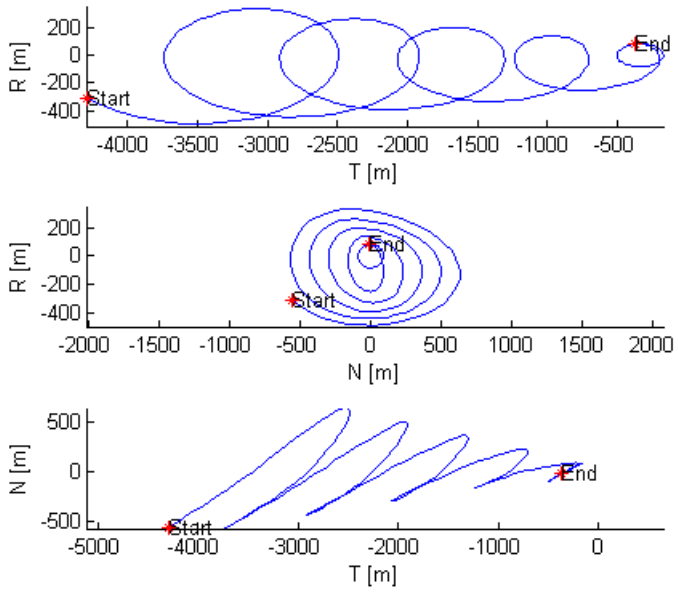

Figure 4. Nominal spiral approach in the absence of errors: projections.

- Mean along-track separation of 300 m: $a\delta\lambda = -300$ m,
- Amplitude of radial oscillations of 80 m: $a\delta e_x = 0$ m, $a\delta e_y = 80$ m.
- Amplitude of cross-track oscillations of 90 m: $a\delta i_x = 0$ m, $a\delta i_y = 90$ m.

Throughout the paper, the relative orbit of the target delivery geometry is shortly also referred to as the *target relative orbit* or the *target ROEs*.

Measurement modeling

In the scope of this GNC simulation, an LOS measurement is a unit vector representing the direction to the Client as seen in the orbital reference frame of the Servicer. Alternatively, LOS can be represented in terms of the azimuth and the elevation of the Client in the orbital frame of the Servicer. The transformation between the camera frame and orbital frame were not considered here as the information on the Servicer attitude and absolute orbit is supposed to be available. For simulation of the measurements, the following major sources of error in azimuth and elevation measurements were considered.[3]

- Side illumination by the Sun. The major factors here are the along-track separation between the two spacecraft, the actual illumination conditions, and the maximum possible lateral error which amounts to half of the Client bus side length (assumed bus side length 2.5 m). In this way, the sideways illumination bias is modeled as

$$\varepsilon_{\mathrm{SI}} = \arctan \frac{1.25 \times F}{\delta r_{\mathrm{T}}},$$

where δr_{T} is the along-track separation and F is a factor which accounts for the changing illumination conditions dependent on the actual Sun-Client-Servicer constellation.

- Image processing noise of about 1 pixel that can be modeled as a normally distributed random variable with a standard deviation of 0.01 degree.

Thus, the side illumination bias and the image processing noise are added to the "ideal" azimuth and elevation of the Client as seen from the Servicer in its orbital reference frame providing "measured" observations.

The scope of the measurement modeling within this simulation is restricted to the simulation of the line of sight (or azimuth and elevation) measurements only. In a real scenario, LOS measurements will be the end product of a complex multi step process of raw image treatment including cluster detection and linking, target identification and the transformation of the image 2D pixel coordinates into a LOS vector.[3] A complete analysis of the image processing aspects related to the far, mid- and close range approach can be found in Reference 3.

Simulation architecture

Figure 5 illustrates the architecture of the simulation environment and the general flow of the proposed GNC algorithm. The most important blocks are described in the following.

- Simulation input (on the left of the diagram):
  - CL_REC: initial position and velocity vector of the Client satellite in form of a GSOC database record, containing initial epoch and the S/C parameters such as mass and cross-sectional areas. Such a database record can also contain maneuvers as time-tagged Delta-Vs.

    It should be mentioned that CL_REC is only used for initialization of the Servicer orbit and propagation of the reference, or "true", Client orbit for measurement simulation and analysis of the accuracies of the estimated ROEs as compared to the "true" ROEs. Obviously, the information on the true Client orbit might not be available in reality; therefore, it was not used during angles-only ROD or maneuver planning.
  - Simulation setup data:
    - N_DRIFT_ORB: number of drift orbits (currently set to 4.5).
    - MAX. INITIAL ROEs ERRORS: a vector of maximum expected errors in ROEs when based on two absolute orbits after an optical tracking OD, currently set to

      $$\varepsilon_{a\delta\boldsymbol{\alpha}}^{\mathrm{OD}} = (21, 450, 100, 100, 300, 300)^T .$$

      Initial OD errors in element $a\delta\boldsymbol{\alpha}(i)$, $i = 1, ..., 6$, are modeled during the initialization as random variables uniformly distributed on the interval

      $$\left[-\varepsilon_{a\delta\boldsymbol{\alpha}}^{\mathrm{OD}}(i), +\varepsilon_{a\delta\boldsymbol{\alpha}}^{\mathrm{OD}}(i)\right] .$$

    - INTERMED. TARGET ROEs: Intermediate target ROEs used for maneuver planning in all the phases except the phase of final correction maneuvers, namely $a\delta\boldsymbol{\alpha}_i = (0, -300, 0, 95, 0, 105)^T$. Slightly higher values as compared to the target delivery geometry for the relative eccentricity and relative inclination vector components allow to improve the safety characteristics until the very end of the far range approach.

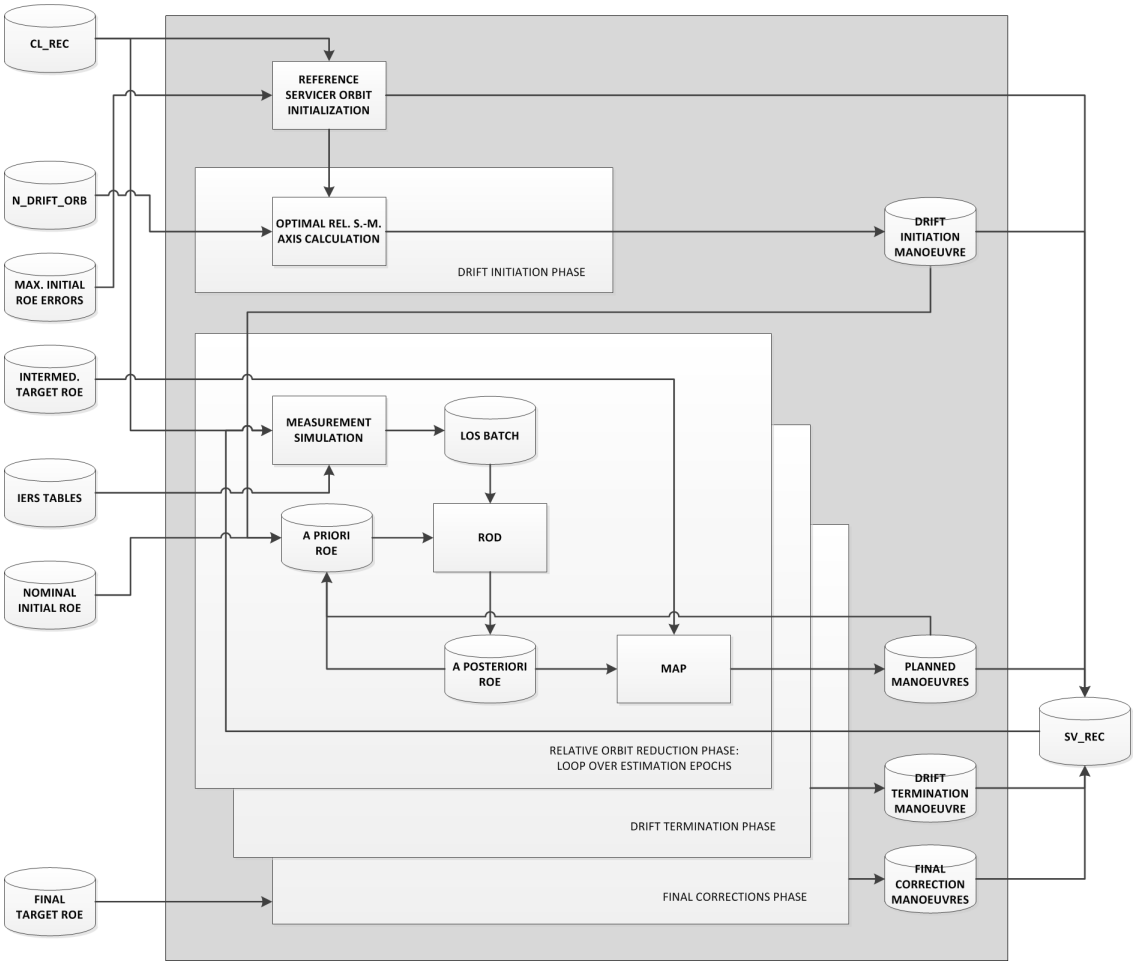

Figure 5. GNC simulation architecture

  - ∗ FINAL TARGET ROEs: ROEs of the nominal delivery geometry at the end of the far range approach are set to $a\delta\boldsymbol{\alpha}_t = (0, -300, 0, 80, 0, 90)^T$.
  - ∗ NOMINAL INITIAL ROEs: ROEs of the initial nominal geometry are currently set to $a\delta\boldsymbol{\alpha}_0 = (0, -3500, 0, 500, 0, 700)^T$.
- – IERS TABLES: Tabular data on leap seconds and polar motion. Required for propagation of the ”true” Servicer and Client orbits for measurement simulation.

- REFERENCE SERVICER ORBIT INITIALIZATION: Pseudo-random initial ROEs errors are generated at this step and added to the nominal initial ROEs. The sum is then ”added” to the initial Client orbit to produce the initial ”true” Servicer orbit in form of a database record SV_REC.

- Drift initialization phase based on the nominal ROEs:

  - – OPTIMAL REL. S.-M. AXIS CALCULATION: Optimal offset between the semi-major axes of the Servicer and the Client is calculated based on the nominal initial and target relative longitude and the selected number of drift orbits.

- DRIFT INITIATION MANEUVER: The optimal argument of latitude for the first reduction of the eccentricity vector is calculated and transformed into optimal maneuver epoch. The epoch and the Delta-V vector constitute a maneuver record, which is appended to SV_REC. The drift termination epoch is also determined at this stage based on N_DRIFT_ORB.

- Relative orbit reduction phase in a loop over epochs of estimation:

  - MEASUREMENT SIMULATION: Initial "true" orbits of the Client and the Servicer are propagated for simulation of the line of sight measurements, which are stored in an array LOS BATCH of a dedicated data type. In the measurement simulations during all phases, the "true" LOS vector is calculated in the orbital frame of the Servicer and transformed into azimuth and elevation of the Client as seen from the Servicer. The side illumination bias and the image processing noise are added as described in the previous section. The resulting "measured" azimuth and elevation are transformed back to a LOS vector, which is then considered to be one of the measurements in the batch. Around 540 LOS measurements spanning ca. 30 hours preceding any ROD epoch are generated (except before the first ROD, where the sampling interval of 20 seconds is used leading to 5400 LOS measurements in the batch).
  - ROD: Relative orbit determination based on batch least squares estimation with a priori information. During the first ROD of the relative ellipse reduction phase, the a priori ROEs are obtained by propagating nominal ROEs with the drift initialization maneuver taken into account. At the later RODs, the a priori information is provided by the ROEs determined for the previous estimation epoch of the relative orbit reduction phase, which are propagated taking into account the planned maneuvers executed between the previous and the current estimation epochs.
  - MAP: Maneuver planning functionality which requires as input the ROEs estimated during the previous step and the target ROEs. Note that at this stage, the intermediate target orbit is used. Optimal relative semi-major axis is calculated based on the currently estimated mean relative longitude, the target mean relative longitude and the remaining time until the drift termination maneuver. The tangential drift correction maneuver is then computed from the difference between the currently optimal relative semi-major axis and the currently estimated relative semi-major axis. This provides a mechanism for drift correction in case of large perturbations on the relative dynamics, e.g. due to solar radiation pressure or maneuver execution errors. The drift correction maneuver is executed directly after the ROD.

    Based on the currently estimated relative mean longitude, the remaining integer number of drift orbits is calculated. After having predicted the effect of the drift termination maneuver on the eccentricity vector, the remaining necessary change in the eccentricity vector is calculated and divided by the number of remaining orbits. This gives the magnitude of the necessary Delta-V per day in the radial direction. Since radial thrust couples the changes of relative eccentricity to the changes of the mean relative longitude, performing only one radial maneuver per day would produce a deviation from the required drift rate. Therefore, the daily Delta-V is split in two maneuvers separated by half a day to keep the relative drift rate constant. The maneuvers are executed at the optimal arguments of latitude.

The inclination vector control concept is similar although somewhat easier. Since inclination control is not coupled to changes in any other ROE, it is performed independently by thrusting in the direction orthogonal to the orbital plane. Again, the currently estimated and the target inclination vectors are used to calculate the total change in the inclination vector yet to achieve, which leads to an estimate of remaining Delta-V necessary in the normal direction. This estimate is divided by the double of the remaining number of drift orbits, to provide the Delta-V of the next two maneuvers separated by half a day. The maneuvers are executed at the optimal arguments of latitude. The resulting 5 time-tagged Delta-Vs (one tangential, two radial and two normal) form a maneuver record and are appended to SV_REC.

- Drift termination phase:

  - MEASUREMENT SIMULATION: Again approximately 540 LOS measurements are simulated based on the propagated CL_REC and SV_REC, spanning 30 hours before the drift termination maneuver.
  - The ROD before the drift termination maneuver uses as a priori information the ROEs determined by the last ROD of the relative orbit reduction phase. These are propagated with RMM to the estimation epoch taking into account the planned maneuvers executed before the estimation epoch.
  - MAP: The difference between the target relative semi-major axis $a\delta a = 0$ and the a posteriori relative semi-major axis gives insight into the necessary magnitude of the tangential drift-stop maneuver. Tagged with the epoch determined already at the drift initialization step, this Delta-V is appended to SV_REC.

- Final corrections phase:

  - Due to the mentioned latency in the improvement of the AON observability properties, the last ROD of the simulation is performed half a day after the drift termination maneuver. Measurements spanning a bit less than 5 hours are simulated with a sampling rate of 200 seconds, leading to 90 LOS measurements in the batch.
  - MAP: The difference between the target relative semi-major axis and the resulting a posteriori relative semi-major axis allows computing the final drift correction maneuver. One final radial and one final normal maneuver are calculated and performed at the closest optimal epochs in the next half a day.

- Simulation output (on the right of the diagram):

  - SV_REC containing the "true" initial Servicer position and velocity vectors, S/C parameters and all the planned maneuvers from the drift initialization to the final correction maneuvers. For navigation performance analysis the reference (or "true") Servicer ephemeris along the approach trajectory are obtained by propagating SV_REC over the planned maneuvers. No maneuver execution errors such as errors in thrust direction or firing duration have been considered in the framework of this simulation.

SIMULATION RESULTS AND ALGORITHM PERFORMANCE ANALYSIS

Angles-only navigation performance

The accuracy of the AON solution was estimated during the whole far range transfer from the relative distances of -3500 m to -300 m towards the Client in flight direction. To assess the influence of the absolute orbit determination errors on the relative AON solution along the trajectory, the OD errors were modeled as random variables uniformly distributed in the range defined by the maximum expected errors of the absolute navigation based on optical tracking measurements.

In total 100 simulations were performed as illustrated in Figure 6. In each of them, pseudo-random errors were generated and added to the nominal initial relative orbital elements. The result was used to initialize the propagation of the "true" Servicer and Client orbits for later analysis of AON performance. At the same time, the nominal initial ROEs were treated as the solution obtained from the absolute navigation and used as a priori information for the first angles-only relative orbit determination. In other words, the difference between the "true" (unknown in real conditions) and "estimated" initial ROEs was modeled as a random vector with components uniformly distributed on the intervals $\left[-\varepsilon^{\mathrm{OD}}_{a\delta\boldsymbol{\alpha}}(i), +\varepsilon^{\mathrm{OD}}_{a\delta\boldsymbol{\alpha}}(i)\right]$, $i = 1, .., 6$, where $\varepsilon^{\mathrm{OD}}_{a\delta\boldsymbol{\alpha}} = (21, 450, 100, 100, 300, 300)^T$, and $\varepsilon^{\mathrm{OD}}_{a\delta\boldsymbol{\alpha}} = \sqrt{2} \times \varepsilon^{\mathrm{OD}}$, $\varepsilon^{\mathrm{OD}}$ are the maximum expected absolute OD errors.

In general, the first ROD can be performed already before the drift-initiation maneuver. In this case the estimates of the relative eccentricity and inclination vectors can receive a slight improvement compared to the estimates based on the absolute navigation. However, in the absence of maneuvers, the problem of angles-only navigation is not fully solvable. In particular, it is not possible to solve for the relative semi-major axis $a\delta a$ and the relative mean longitude $a\delta\lambda$.

This major issue inherent to angles-only navigation is referred to as non-observability of the complete AON problem.[8] The reason of this issue is that an infinite number of relative orbits produce the same LOS measurements, and therefore, to achieve the complete observability a maneuver is necessary that produces a change in the line of sight not aligned with the instantaneous direction of the natural LOS profile. Therefore, in the suggested control strategy, the first ROD is performed after the drift initiation maneuver.

The first ROD following the drift initiation maneuver solves with sufficient accuracy for the relative inclination vector. Typically, the remaining error is less than ± 40 meters in $a\delta i_x$ and less than ± 150 meters in $a\delta i_y$. The improvement in the estimated $a\delta e_x$ and $a\delta e_y$ is less apparent as the estimated relative eccentricity vector is exposed to the strong periodic perturbations due to the forces that are taken into account in the propagation of the "true" orbits, but neglected in the AON model filter.

The relatively large tangential drift-initiation maneuver improves the observability properties of the AON problem which can be observed in the steep reduction of the error in $a\delta a$ around 0.7-0.8 days of simulation time (ca. 18 hours after the drift initiation). After that the distribution of the errors in the relative semi-major axis remains rather constant due to the absence of large changes in line of sight towards Client. The second significant improvement in the estimate of $a\delta a$ happens with the final ROD performed half a day after the drift termination maneuver.

During the relative orbit reduction phase, the quality of the estimates of the relative eccentricity and inclination vector continuously improves. Also the mean relative longitude $a\delta\lambda$ receives a gradual improvement along the trajectory. The accuracies of the AON solutions along the approach are summarized in Table 1, where the values refer to the worst-case scenario. It should be mentioned

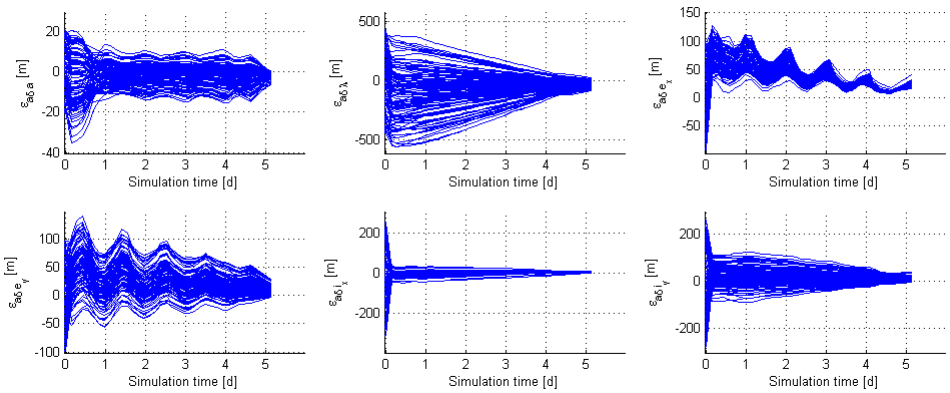

Figure 6. Errors in AON solutions for 100 simulations

that along the approach the errors in ROEs are normally not centered around zero. Thus, much smaller dispersions around the mean error values can be expected.

Table 1. Summary of worst-case (maximum) ROD errors along the approach (DI: Drift Initiation; DT: Drift termination); unit: meter

Approach phase	$a\delta a$	$a\delta\lambda$	$a\delta e_x$	$a\delta e_y$	$a\delta i_x$	$a\delta i_y$
Before 1st ROD (optical OD errors)	< 21	< 450	< 100	< 100	< 300	< 300
After 1st ROD (ca. 15 min after DI)	< 35	< 550	< 120	< 150	< 40	< 150
After 5th-7th ROD (ca. 18 hrs after DI)	< 15	< 530	< 100	< 100	< 40	< 120
Last ROD before DT	< 15	< 120	< 25	< 55	< 15	< 40
Final ROD after DT	< 7	< 80	< 40	< 30	< 10	< 40

Guidance and control performance

The results of the performed 100 simulations under variation of the initial absolute OD errors in ROEs are presented in Figure 7 and Figure 8. Figure 7 shows clearly how ROEs, spread initially on the interval determined by the maximum expected optical OD errors, converge to the target ROEs. The middle plot of Figure 8 demonstrates that the safety threshold of 50 m in the plane perpendicular to the flight direction is never violated, i.e. the Servicer never enters the collision avoidance region around the Client (depicted with a red circle), which guarantees the safety of the formation during the whole transfer. The minimum relative distance in the RN-plane among the 100 performed simulations is 53.5 meters. Table 2 provides a summary of the achieved accuracies in final ROEs (end of day 6) with respect to the nominal target ROEs.

Table 2. Summary of achieved final ROEs accuracies; unit: meter

ROEs	$a\delta a$	$a\delta\lambda$	$a\delta e_x$	$a\delta e_y$	$a\delta i_x$	$a\delta i_y$
Mean offset with respect to the target ($\bar{\varepsilon}$)	0.97	9.54	-20.69	-10.96	-3.41	-10.16
Mean absolute deviation from the mean offset ($\overline{\boldsymbol{D}}$)	1.16	49.02	2.34	6.08	0.61	8.58

In Table 2, mean offset with respect to the target refers to the mean error in final ROEs with

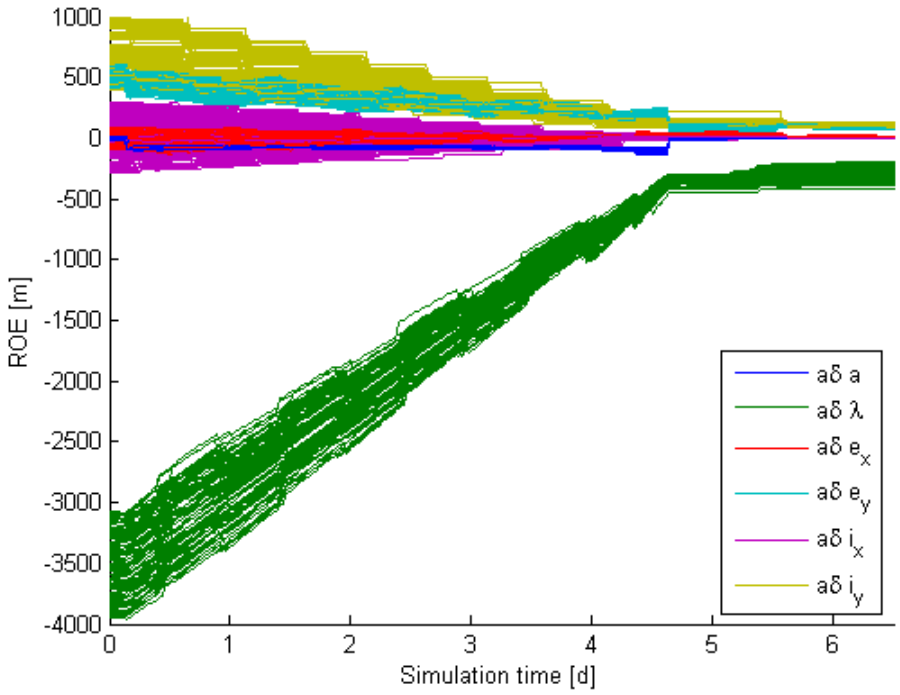

Figure 7. Evolution of the "true" ROEs during far range approach (100 simulations)

respect to the target ROEs of the nominal delivery geometry, calculated as

$$\overline{\boldsymbol{\varepsilon}} = a\delta\boldsymbol{\alpha}_t - \overline{a\delta\boldsymbol{\alpha}_f}, \quad \overline{a\delta\boldsymbol{\alpha}_f} = \frac{1}{N}\sum_{j=1}^{N} a\delta\boldsymbol{\alpha}_f^j.$$

Here the summation is performed over the simulations indexed with j, and $N = 100$. Final achieved elements for simulation j are denoted by $a\delta\boldsymbol{\alpha}_f^j$, while the nominal target elements are denoted by $a\delta\boldsymbol{\alpha}_t$.

In Table 2, mean absolute deviation from the mean offset refers to

$$\overline{\boldsymbol{D}} = \frac{1}{N}\sum_{j=1}^{N} |\overline{a\delta\boldsymbol{\alpha}_f} - a\delta\boldsymbol{\alpha}_f^j|,$$

which provides a measure of the distribution of the errors around their mean values.

Delta-V budget

The nominal approach trajectory and the presented coupled guidance and control algorithm was designed on the basis of a trade-off analysis of the total Delta-V consumption, transfer duration and the fulfillment of the safety constraints. Figure 9 illustrates the dependency of the total Delta-V "spent" during the approach on the total required change in a particular relative orbital element. While the first three plots do not reveal any clear dependency, the plot in the lower right corner

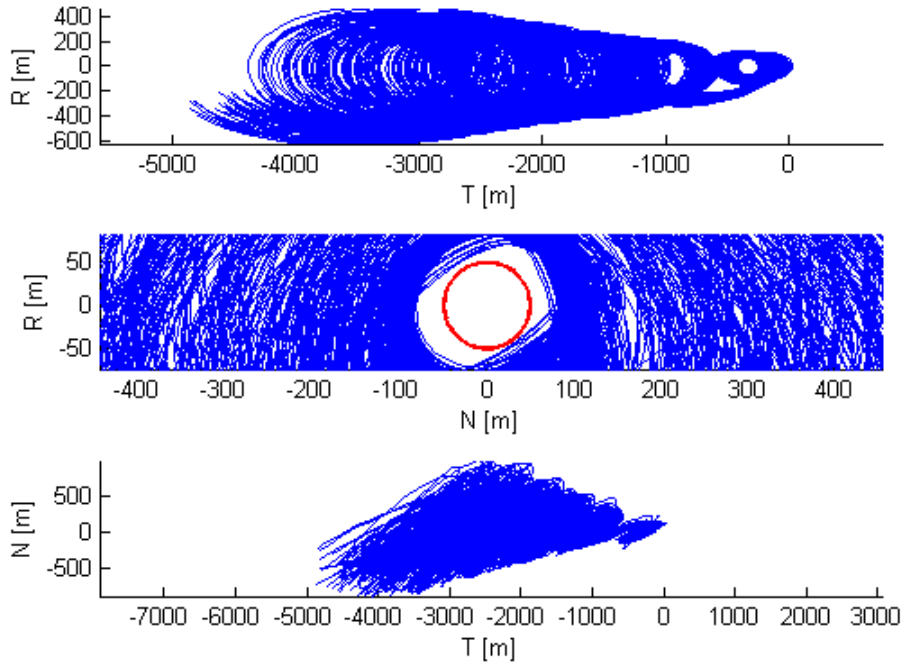

Figure 8. Projection of the "true" relative position of the Servicer with respect to the Client in the orbital reference frame (100 simulations)

demonstrates a very pronounced linear relation between the required change in the magnitude of the inclination vector and the total Delta-V "consumed" during the approach.

Two characteristics of the required Delta-V capabilities can be outlined. First, the far range approach towards a target in near-GEO can be regarded as a low-cost activity in terms of required fuel. Second, for the performed 100 simulations, the final total absolute Delta-V varies between 0.05 and 0.11 m/s, while the typical maneuver size is of the order of a few millimeters per second.

CONCLUSIONS

The paper presents a prototyped novel GNC algorithm covering all major flight dynamics aspects of a far range approach towards a target in near-geostationary orbit, where on-orbit servicing applications are considered as a baseline scenario. For validation of the suggested strategy, 100 simulation runs were performed under varying initial conditions corresponding to the absolute orbit determination uncertainty prior to the approach initiation. Simulated line of sight measurements of a typical far range optical camera with a FOV of 10 degrees provide the ground for angles-only navigation.

The results of the performed simulations prove the feasibility of a safe approach towards the Client up to the relative distance where a transition from the far range camera to the mid-range camera is possible in a time non-critical manner. Moreover, the Servicer never enters a collision avoidance region defined around the Client in the plane orthogonal to the flight direction, which

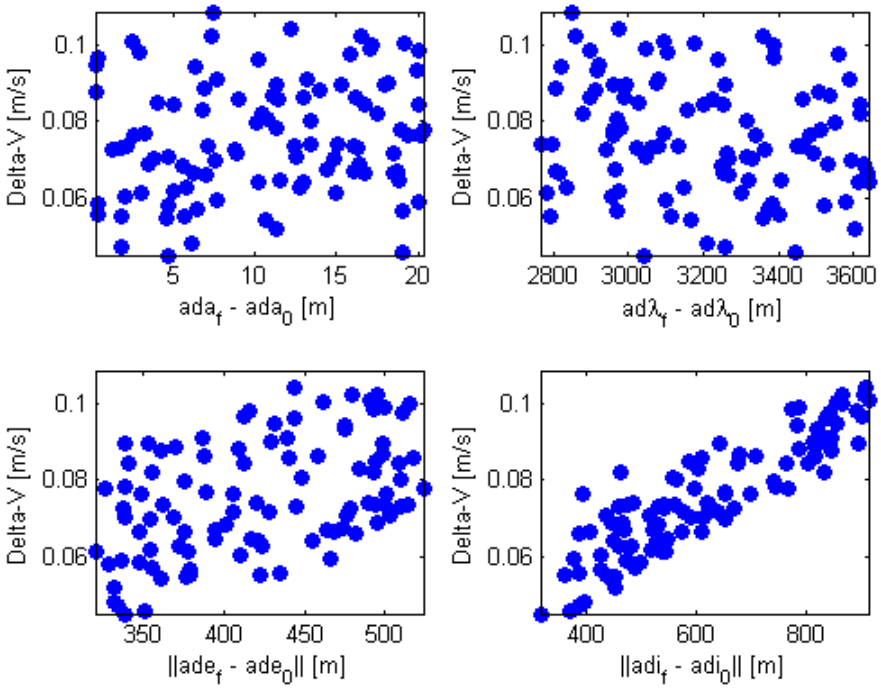

Figure 9. Total absolute Delta-V required for the far range approach (100 simulations)

guarantees the safety of the formation at any time.

Due to the low Delta-Vs required for the far range approach campaign, and the small magnitudes of each of the separate maneuvers, low thrust propulsion systems could potentially be of interest in the scope of the algorithm applications to on-orbit servicing in GEO.

REFERENCES

[1] Ardaens, J.-S., D'Amico, S., Fischer, D.: Early flight results from the TanDEM-X autonomous formation flying system, 4th International Conference on Spacecraft Formation Flying Missions and Technologies (SFFMT), St-Hubert, Quebec (2011)

[2] Ardaens, J.-S., Kahle, R., Schulze, D.: In-flight performance validation of the TanDEM-X autonomous formation flying system, 5th International Conference on Spacecraft Formation Flying Missions and Technologies (SFFMT), Munich, Germany (2013)

[3] Benninghoff, H. and Boge, T.: A Novel Navigation and Sensor Strategy for Far, Mid and Close Range Rendezvous to a Cooperative Geostationary Target Spacecraft, AIAA SPACE 2015 Conference and Exposition, Pasadena, California.

[4] Clohessy, W.H., Wiltshire, R.S.: Terminal guidance system for satellite rendezvous. J. Aerosp. Sci. 27(9), pp. 653-658 (1960)

[5] D'Amico, S.: Autonomous formation flying in low earth orbit, Technical University of Delft, (2010)

[6] D'Amico, S., Ardaens, J.-S., Larsson, R.: Spaceborne autonomous formation-flying experiment on the PRISMA mission. J. Guid. Control Dyn. 35(3), pp. 834-850 (2012)

[7] D'Amico, S., Ardaens, J.-S., Gaias, G., Benninghoff, H., Schlepp, B., Jørgensen, J.L.: Noncooperative rendezvous using angles-only optical navigation: system design and flight results. J. Guid. Control Dyn. 36(6), pp. 1576-1595 (2013)

[8] Gaias, G., D'Amico, S., Ardaens, J.-S.: Angles-only Navigation to a Non-Cooperative Satellite using Relative Orbital Elements, Astrodynamics Specialists Conference AAS, 13-16 August 2012, Minneapolis, MN, USA

[9] Gaias, G., Ardaens, J.-S., D'Amico, S.: The Autonomous Vision Approach Navigation and Target Identification (AVANTI) experiment: objectives and design, 9th International ESA Conference on Guidance, Navigation & Control Systems, Porto, Portugal (2014)

[10] Montenbruck, O., Gill, E.: Satellite orbits: Models, Methods and Applications, Springer Verlag, Heidelberg (2000)

[11] Montenbruck, O., Kirschner, M., D'Amico, S., Bettadpur, S.: E/I-vector separation for safe switching of the GRACE formation. Aerosp. Sci. Technol. 10(7), pp. 628-635 (2006)

[12] Spiridonova, S., Kahle, R.: Relative orbit dynamics in near-geostationary orbit, 25th International Symposium on Space Flight Dynamics, 19-23 October, 2015.

[13] Weigel, M., Fiedler, H., Siminski, J. Meinel, M., Basermann, A., Schildknecht, T., Plonner, M.: Erste Version des Bahnkataloges BACARDI - Ergebnisse einer Testkampagne zur Überwachung geostationären Objekte. DWT 4. Formum Weltraum, 09.-10. Sept. 2014, Bad Godesberg, 2014